A Microscopic Investigation into the Capacity Drop: Impacts of the Bounded Acceleration and Reaction Time

Yuan, Kai; Knoop, Victor; Hoogendoorn, Serge

Publication date
2016

Document Version
Accepted author manuscript

Published in
Transportation Research Record

A MICROSCOPIC INVESTIGATION INTO THE CAPACITY DROP: IMPACTS OF BOUNDED ACCELERATION AND REACTION TIME

Kai Yuan, PhD candidate
TRAIL research school
Department of Transport and Planning
Faculty of Civil Engineering and Geosciences
Delft University of Technology
Stevinweg 1, P.O. Box 5048, 2600 GA Delft, The Netherlands
Phone: +31 15 278 1384
Email: k.yuan@tudelft.nl

Victor L. Knoop, Assistant Professor
Department of Transport and Planning
Faculty of Civil Engineering and Geosciences
Delft University of Technology
Stevinweg 1, P.O. Box 5048, 2600 GA Delft, The Netherlands
Phone: +31 15 278 8413
Email: v.l.knoop@tudelft.nl

Serge P. Hoogendoorn, Professor
Department of Transport and Planning
Faculty of Civil Engineering and Geosciences
Delft University of Technology
Stevinweg 1, P.O. Box 5048, 2600 GA Delft, The Netherlands
Phone: +31 15 278 5475
Email: s.p.hoogendoorn@tudelft.nl

July 2015

Word count

nr of words in abstract	201
nr of words in manuscript (including abstract and references)	5545
nr of figures & tables	7
total	7496

ABSTRACT

The capacity drop indicates that the queue discharge rate is lower than the free-flow capacity. Studies show that queue discharge rates vary under different traffic conditions. Empirical data show that the queue discharge rate increases as the speed in congestion increases. Insights into the underlying behavioral mechanisms that result in such variable queue discharge rates can help minimize traffic delays and eliminate congestion. However, to the best of the authors' knowledge, few efforts have been devoted to testing impacts of traffic behaviors on the queue discharge rate. This paper tries to fill this gap. We investigate to what extent the acceleration spread and reaction time can influence the queue discharge rate. It is found that the (inter-driver) acceleration spread does not reduce the queue discharge rates as much as found empirically. Modelling reaction time might be more important than modeling acceleration for capacity drop in car-following models. A speed-dependent reaction time mechanism for giving variable queue discharge rates is proposed. That is, decreasing reaction time as the speed in congestion increases can give the same queue discharge rate as found empirically. This research suggests that motivating drivers to speed up earlier could increase the queue discharge rate and thereby minimize delays.

1. INTRODUCTION

Road congestion can be categorized into two classes: standing queues with heads fixed at a bottleneck and stop-and-go waves with queue fronts moving upstream. The bottleneck is a fixed point where the congestion head is located. Once congestion sets in, the flow out of congestion is the queue discharge rate. This flow is generally lower than the free-flow capacity, i.e., the maximum flow. This phenomenon is called the capacity drop.

The magnitude of the capacity drop is not constant. Empirical data show that the queue discharge rate vary considerably at the same location [1, 2]. This is shown to correlate well with congestion states [3, 4]. Yuan et al. [3] reveal a linear relation between the speed in congestion and the queue discharge rate (see Figure 1). The specific relation is based on empirical data collected on freeway A4 and A12 in the Netherlands. Road design and control measures can contribute to varying queue discharge rates [5, 6]. These findings show that there might be promising strategies that can increase the queue discharge rate to reduce delays. However, to determine effective approaches, an insight is needed into the underlying behavioral mechanisms that cause the capacity drop. Therefore, this paper tries to investigate the impacts of driver behavior on the queue discharge rate.

More specifically, this paper studies the impacts of acceleration and reaction time on the queue discharge rate. The acceleration can give the capacity drop with inter-driver acceleration spread. Inter-driver acceleration spread (or in short: acceleration spread) means that vehicles do not have the same acceleration. As a result, voids will be created between a low-acceleration vehicle and its high-acceleration predecessor. The reaction time indicates how long a following vehicle needs to take to react to the change of its leader's driving behavior. Voids can also be created if the follower's reaction time is longer than Newell's reaction time (see section 3.3). In this paper, we call such long reaction time the extended reaction time. To what extent the inter-driver acceleration spread and the extended reaction time contribute to the capacity drop is unknown. Hence, we here study the impacts of the acceleration spread and the extended reaction time on the queue discharge rate.

This paper develops analytical models to investigate the independent impact of accelerations and reaction time. Furthermore, we design numerical experiments for two objectives. First, the experiment is used to validate the analytical model to ensure the approximation in the model is accurate enough. Second, we use the experiment to see the combination effects of acceleration spread and reaction time on the queue discharge rate. The empirical relation revealed in [3] is the reference used in our analyses, see Figure 1.

Our study excludes several factors that may influence the queue discharge rate. Firstly, drivers' perspectives, i.e., whether drivers are aggressive or timid, are excluded. Secondly, lane changing is not considered in this paper. As argued in [7], if we simulate a stop-and-go wave moving on a homogeneous road section, lane changing frequency should be very low in an acceleration mode.

The outline of the paper is as follows: we start with a literature review in section 2. Then section 3 presents the analytical investigation on the capacity drop. In section 4, we use simulations to validate the analytical model (section 4.2) and investigate the combination of acceleration and reaction time (section 4.3), followed by discussions and conclusions in section 5.

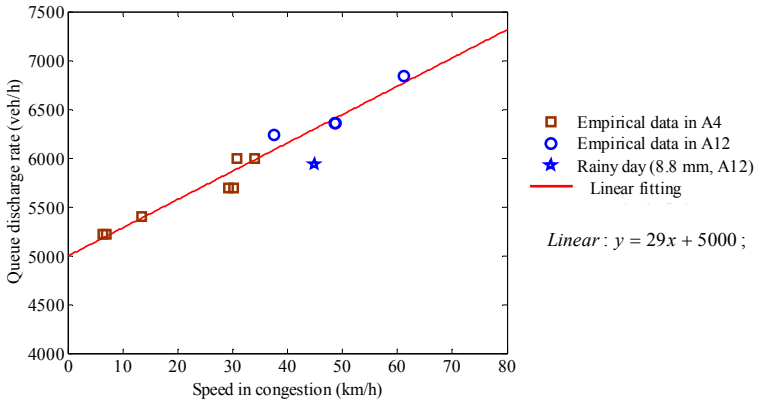

Figure 1 Relation between queue discharge rate and the speed in congestion [3].

2. LITERATURE REVIEW

A wide range of capacity drop values have been observed, which are reviewed in section 2.1. The wide range of the capacity drop values could be due to various queue discharge rates which correlate well with different congested states. The research objective of this paper is to investigate the relation between driving behavior and the queue discharge rate. Hence, section 2.2 reviews previous traffic behavioral mechanism of the capacity drop.

2.1 Empirical features of the capacity drop

The capacity drop was reported for the first time in 1991, with a drop of 6% [8] and 3% [9]. In the past decades, the capacity drop have been studied more often, with values of the drop ranging between 3% and 18% [6]. In [10] the capacity drop ranges from 8% to 10%. In [5] the capacity falls by 15% at an on-ramp bottleneck. Chung et al. [1] show a range of capacity drop from 3% to 18% with data collected at three active bottlenecks, which shows a drop from 8% to 18% at the same location. Cassidy and Rudjanakanoknad [11] observe capacity drop between 8.3% and 14.7%.

We argue that the wide range of capacity drop values in literature correlates well with the congestion state. Yuan et al. [3] show a positive correlation between the queue discharge rate and the speed in congestion with empirical data collected on freeways in the Netherlands. Oh and Yeo [4] find that the queue discharge rate is related to the severity of congestion by analyzing microscopic trajectory data. Hence, the research question is: what is the mechanism behind the dependency of discharge rate on the congested states? Answering this question might help to better understand the microscopic mechanism of the capacity drop.

2.2 Overview of assumptions on mechanisms of the capacity drop

Many studies have been reporting the capacity drop in the past decades. Table 1 summarizes most of the existing most popular assumptions on the traffic behavioral mechanism of capacity drop. Generally, we can divide them into three categories: bounded acceleration capability, inter-driver/vehicle spread, and intra-driver spread.

Bounded acceleration capability means vehicles cannot accelerate instantaneously. Consequently lane change manoeuvers can create voids in the traffic stream. The limited acceleration causes that the lane changing vehicle cannot catch up with its new predecessor [12-14]. Coifman and Kim [15] show that lane changing in the far downstream of the congestion can result in the capacity drop, too. Insertions result in shockwaves in the new lane and the divergences in the old lane create voids which cannot be filled in duo to the bounded acceleration capability. So an aggregated flow detected in the downstream of queue could be lower than the capacity.

Inter-driver/vehicle spread indicates the spread of drivers and vehicles. Papageorgiou et al. [7] state that the capacity drop is due to the acceleration difference between two successive vehicles. Voids can be created between a low-acceleration vehicle and its high-acceleration predecessor. Chen et al. [16] try to explain the capacity drop in a view of drivers' perspectives. Wong and Wong [17] reproduce the capacity drop when modeling the multi-class traffic flow.

Table 1 Possible mechanisms of the capacity drop

Basic mechanisms	Assumptions on mechanisms:	References:
a) Bounded acceleration capability	Lane changing	Laval and Daganzo [12] Leclercq et al. [13] Leclercq et al. [14] Coifman and Kim [15] Coifman et al. [18]
b) Inter-driver/vehicle spread	Drivers' perspective	Chen et al. [16]
	Acceleration variance	Papageorgiou et al. [7]
	Multi-class vehicles	Wong and Wong [17]
c) Intra-driver spread	Variance-driven time headways	Treiber et al. [19]
	Multiphase car-following theory	Zhang and Kim [20]
	Asymmetric driving behavior theory	Yeo [21]
	Activation level	Tampère [22]

The third popular explanation, intra-driver spread, assumes driver behaviors vary depending on traffic conditions. Treiber et al. [19] assume drivers would choose a longer time headway in congestion than that in free flow. The preferred time headway in congestion increases as density increases. This assumption, also called variance-driven time headways, is based on an empirical observation of an increasing time gaps between one vehicle's front bumper and the rear bumper of the preceding vehicle after a considerable queuing time in [23]. Zhang and Kim [20] propose a multi-phase car-

following traffic flow theory to reproduce the capacity drop. They highlight that the capacity drop is a result of driver behavior spread across three phases, i.e., acceleration, deceleration and coasting. Yeo [21] validates the acceleration and deceleration curves to further develop the asymmetric microscopic traffic flow theory based on empirical trajectory data, explaining the capacity drop as a difference of the maximum flow between the acceleration and the deceleration curve in density-flow fundamental diagram. The asymmetric driver behavior theory is also applied in [4] to understand the impacts of stop-and-go waves on the capacity drop. Tampère [22] assumes drivers' behavior depends on a temporary, traffic condition dependent variable "activation level". The low activation level used to accounted for a loss of motivation. They reproduce the capacity drop as a result of low activation level in case studies.

In this paper, we focus on studying the impacts of acceleration spread and reaction time on the queue discharge rate and its correlation with the congestion state.

3. ANALYTICAL INVESTIGATION

This section analytically investigates to what extent the acceleration spread (3.1) and reaction time extension (section 3.2) can independently account for the capacity drop. In each of section 3.1 and section 3.2, we firstly present a numerical expression of the queue discharge rate, followed by analysis of the model properties.

Using mathematical derivations show that including acceleration spread in car-following models does not give sufficient capacity drop compared to empirical observations, and that intra-driver reaction time extension mechanism can model similar queue discharge rates as reality. For practical purpose, these conclusions indicate that pushing slowly driving vehicles to speed up earlier, rather than managing vehicular acceleration, might be an approach for minimizing capacity drops and delays.

3.1 Capacity drop due to accelerations spread

In this section we derivate analytical formula for the capacity drop in section 3.1.1 and find the acceleration spread does not give sufficient queue discharge rate reduction compared to empirical observations in section 3.1.2.

3.1.1 Analytical expressions of queue discharge rates

Let us consider a stop-and-go wave moving upstream on a homogeneous road section shown as the grey block in Figure 2. Bold lines are vehicular trajectories. The traffic in the scenario is described by a triangular fundamental diagram with positive wave speed w, free-flow speed v_f and capacity C. The critical density and maximum jam density are given by ρ_{cri} and ρ_{jam}, respectively. There are n vehicles in total in the queue in a single lane, obeying the first-in-first-out (FIFO) rule. Each vehicle is numbered $i\left(i=1,2,...,n\right)$, increasing from the head of the queue $\left(i=1\right)$ to the tail $\left(i=n\right)$. The speed and density in the queue are v_q and ρ_q, respectively. When all vehicles reach the free-

flow speed after leaving the queue, the free-flow spacing and time headway between vehicle i and $i-1$ is given by s_i and h_i, respectively. The minimum free-flow spacing $s_{\min}$ for all vehicles should be $\frac{1}{\rho_{\text{cri}}}$ (or the minimum time headway $h_{\min}=\frac{1}{C}$), indicating no capacity drop at all. Each vehicle i is described by two constants, its desired acceleration a_i^{desire} and acceleration a_i. In principle, every vehicle accelerates with its desired acceleration. However, s_i is at the low end bounded by $s_{\min}$. Therefore, if $a_i=a_i^{\text{desire}}$ will result in $s_i<s_{\min}$, we set $a_i<a_i^{\text{desire}}$ to ensure $s_i=s_{\min}$, Note that $a_1=a_1^{\text{desire}}$. Desired accelerations fall within the interval $[a_{\min},a_{\max}]$. The reaction time of vehicle i is denoted as t_r. All vehicles have reached free-flow speed at x_1 where The sum of free-flow time headways from the second vehicle to the last vehicle is denoted as H.

If all vehicles follows continuous Newell car-following model [24], constructed by shifting its predecessor's trajectory by spacing $\Delta s=\frac{1}{\rho_{\text{jam}}}$ and time $\Delta t=\frac{\Delta s}{w}=\frac{1}{w\rho_{\text{jam}}}$, see Figure 2a, there is no capacity drop, $q_d=\frac{n-1}{H}=\frac{n-1}{(n-1)h_i}=C$.

It is impossible that all vehicles have the same acceleration. We assume the desired acceleration follows an uniform distribution bounded by $a_{\min}$ and $a_{\max}$, i.e., $a^{\text{desire}}\sim U[a_{\min},a_{\max}]$. We exclude the impact of reaction time extensions by setting $\Delta t_{ex}=0\text{s}$. When the desired acceleration of vehicle i is higher than its leader's acceleration, setting $a_i=a_{i-1}$ ensures the follower can neither overtake nor be too close $(s_i<s_{\min})$ to its leader. Otherwise, $a_i=a_i^{\text{desire}}$. In summary,

$$a_i=\begin{cases}a_{i-1} & ,\ a_i^{\text{desire}}>a_{i-1}\\ a_i^{\text{desire}} & ,\ \text{otherwise}\end{cases}=\min\left(a_{i-1},a_i^{\text{desire}}\right) \tag{1}$$

A void is created between two successive vehicles if the follower's desired acceleration is lower than the predecessor's acceleration. In Figure 2c, a dashed line is the Newell trajectory of vehicle i. Note the void between the Newell trajectory and the trajectory of vehicle i. The void means the free-flow spacing is extended by $s_i^{\text{extension}}$:

$$s_i^{\text{extension}}=\frac{\left(v_j-v_f\right)^2\cdot\left(a_{i-1}-a_i\right)}{2a_{i-1}a_i}=\frac{1}{2}\left(v_j-v_f\right)^2\cdot\left(\frac{1}{a_i}-\frac{1}{a_{i-1}}\right) \tag{2}$$

Now let us consider n vehicles within a stop-and-go wave as in Figure 2d. The queue discharge rate q_d is expressed as:

$$q_d=\frac{n-1}{H} \tag{3}$$

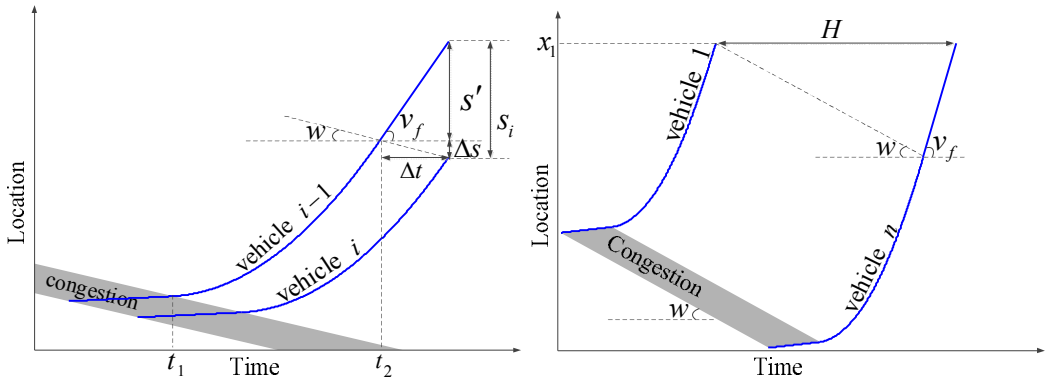

(a) Two vehicles, no capacity drop

(b) n vehicles, no capacity drop

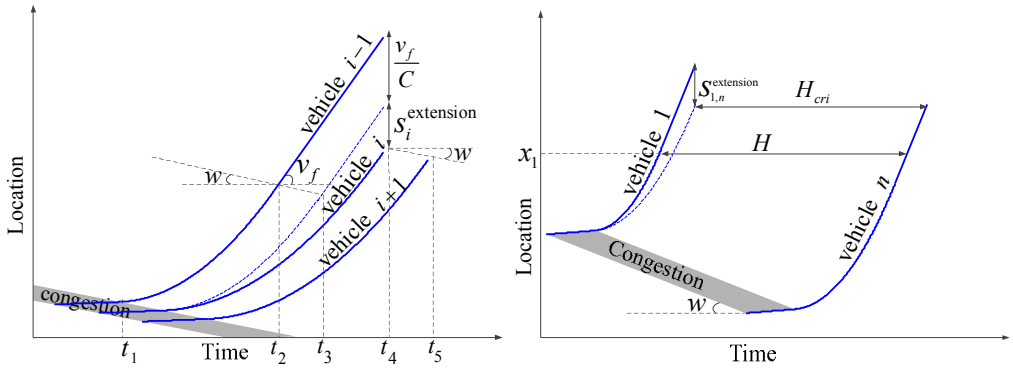

(c) Spacing extensions due to acceleration variability

(d) Queue discharge rates measurements with acceleration variability.

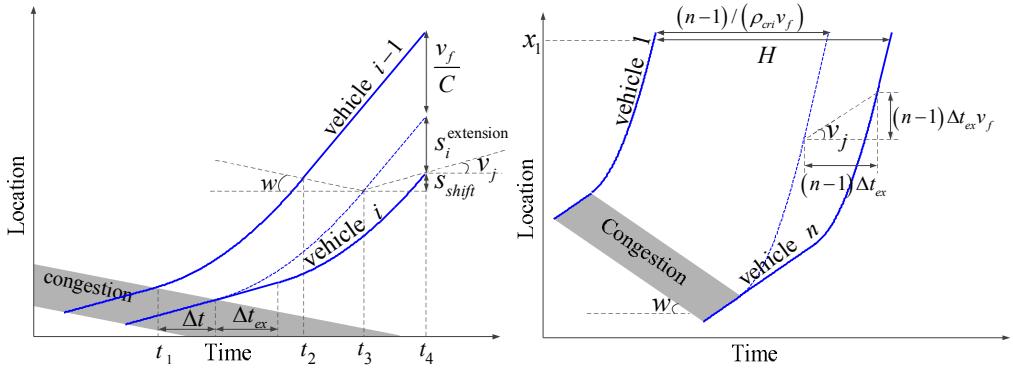

(e) Spacing extensions due to reaction time extensions

(f) Queue discharge rates measurements with reaction time extensions

Figure 2 Measurements of queue discharge rates

We firstly assume the first vehicle has the same acceleration as the last vehicle, see the dashed line in Figure 2d. There is no capacity drop, $H_{\text{cri}} = \frac{n-1}{C}$. Next, we relax such assumption by setting $a_1 = a_1^{\text{desire}} \in U[a_{\min}, a_{\max}]$. An extenstion of spacing $s_{1,n}^{\text{extention}}$ that denotes the free-flow spacing between the first hypothezied trajectory and the first vehicle's trajectory can be estimated in Equation (2). Hence, we have:

$$H = H_{\text{cri}} + \frac{s_{1,n}^{\text{extention}}}{v_f} = \frac{n-1}{C} + \frac{1}{2v_f}\left(v_j - v_f\right)^2 \cdot \left(\frac{1}{a_n} - \frac{1}{a_1}\right) \tag{4}$$

We are interested in the average headway, but since the acceleration of the first and the last vehicle are stochastic, we compute the expected value of H:

$$\begin{aligned} E(H) &= \frac{n-1}{C} + \frac{1}{2v_f}\left(v_j - v_f\right)^2 \cdot E\left(\frac{1}{a_n} - \frac{1}{a_1}\right) \\ &= \frac{n-1}{C} + \frac{1}{2v_f}\left(v_j - v_f\right)^2 \cdot \left(E\left(\frac{1}{a_n}\right) - E\left(\frac{1}{a_1}\right)\right) \end{aligned} \tag{5}$$

Since $a_1 = a_1^{\text{desire}} \in U[a_{\min}, a_{\max}]$, the expected value of $\frac{1}{a_1}$ is:

$$E\left(\frac{1}{a_1}\right) = \frac{\ln\left(\frac{a_{\max}}{a_{\min}}\right)}{a_{\max} - a_{\min}} \tag{6}$$

Now we need $E\left(\frac{1}{a_n}\right)$. Equation (1) indicates that the last vehicle always has the slowest acceleration mong all vehicles:

$$a_n = \min\left(a_{n-1}, a_n^{\text{desire}}\right) = \min\left(a_{n-m}, a_{n-m+1}^{\text{desire}}, ..., a_{n-1}^{\text{desire}}, a_n^{\text{desire}}\right) \tag{7}$$

We choose m from set $[1, n-1]$. Let $\left(a_{(1)}^{\text{desire}}, ..., a_{(n)}^{\text{desire}}\right)$ denote the corresponding order statistics of the random sample $\left(a_1^{\text{desire}}, ..., a_n^{\text{desire}}\right)$ so that $a_{(1)}^{\text{desire}} \le a_{(2)}^{\text{desire}} \le \cdots \le a_{(n)}^{\text{desire}}$. So Equation (7) means $a_n = a_{(1)}^{\text{desire}}$. Hence, the probability density function of a_n equals to the probability density function of the smallest order statistic $a_{(1)}^{\text{desire}}$. According to the order statistic [25], the probability distribution function f_A of $a_{(1)}^{\text{desire}}$ is:

$$f_A\left(a^{\text{desire}}\right) = n\left(1 - F\left(a^{\text{desire}}\right)\right)^{n-1} f\left(a^{\text{desire}}\right) \tag{8}$$

$F\left(a^{\text{desire}}\right)$ and $f\left(a^{\text{desire}}\right)$ are the cumulative distribution function and probability distribution function of the desired acceleration:

$$F\left(a^{\text{desire}}\right) = \frac{a^{\text{desire}} - a_{\min}}{a_{\max} - a_{\min}}, \quad \text{for} \quad a^{\text{desire}} \in \left[a_{\min}, a_{\max}\right] \tag{9}$$

$$f\left(a^{\text{desire}}\right) = \frac{1}{a_{\max} - a_{\min}}, \quad \text{for} \quad a^{\text{desire}} \in \left[a_{\min}, a_{\max}\right] \tag{10}$$

Hence, incorporating Equation (9) and (10) into Equation (11) gives the probability density function f_N of a_n :

$$f_N(a_n)=\left(\frac{a_{\max}-a_n}{a_{\max}-a_{\min}}\right)^{n-1}\frac{n}{a_{\max}-a_{\min}},\ \text{for}\ a_n\in[a_{\min},a_{\max}] \tag{11}$$

We estimate the second-order approximation of $E(g(a_n))$ with the Delta method. Setting Function $g(x)$ as the inverse of x , i.e., $g(x)=\frac{1}{x}$, we can have $E\left(\frac{1}{a_n}\right)=E(g(a_n))$. Thus,

$$E(g(a_n))\approx g(E(a_n))+\frac{1}{2}g''(E(a_n))\sigma^2(E(a_n)) \tag{12}$$

$\mathrm{E}(a_n)$ and $\sigma^2(a_n)$ are the expected value and the standard spread of a_n , respectively. They can be deduced from Equation (11):

$$E(a_n)=\frac{a_{\max}+a_{\min}\cdot n}{1+n} \tag{13}$$

$$\sigma^2(a_n)=\frac{n(a_{\max}-a_{\min})^2}{(2+n)}+\frac{a_{\max}^2(-n+1)+2a_{\min}a_{\max}n}{(1+n)}-\frac{(a_{\max}+a_{\min}\cdot n)^2}{(1+n)^2} \tag{14}$$

Because $g''(E(a_n))=2\cdot\left(\frac{1+n}{a_{\max}+a_{\min}\cdot n}\right)^3$, combining Equation (12)~(14) gets:

$$E(g(a_n))\approx\frac{1+n}{a_{\max}+a_{\min}n}+\left(\frac{1+n}{a_{\max}+a_{\min}n}\right)^3\left(\frac{n(a_{\max}-a_{\min})^2}{(2+n)}+\frac{a_{\max}^2(-n+1)+2a_{\min}a_{\max}n}{(1+n)}-\frac{(a_{\max}+a_{\min}n)^2}{(1+n)^2}\right) \tag{15}$$

Incoporating Equation (6) and Equation (15) into Equation (4), we get the expected value of H :

$$E(H)=\frac{n-1}{C}+\frac{(v_j-v_f)^2(1+n)}{2v_f(a_{\max}+a_{\min}\cdot n)}-\frac{(v_j-v_f)^2\ln\left(\frac{a_{\max}}{a_{\min}}\right)}{2v_f(a_{\max}-a_{\min})}+\frac{(1+n)^3(v_j-v_f)^2}{2v_f(a_{\max}+a_{\min}n)^3}\left(\frac{n(a_{\max}-a_{\min})^2}{(2+n)}+\frac{a_{\max}^2(-n+1)+2a_{\min}a_{\max}n}{(1+n)}-\frac{(a_{\max}+a_{\min}n)^2}{(1+n)^2}\right) \tag{16}$$

This gives get the expected value of the queue discharge rate:

$$E(q_d)=\frac{n-1}{E(H)} \tag{17}$$

3.1.2 Analysis of model properties

We set a triangular fundamental diagram with $w = 18$ km/h, $v_f = 114$ km/h, $C = 6840$ veh/h, $\rho_{\text{cri}} = 60$ veh/km and $\rho_{\text{jam}} = 440$ km/h. This fundamental diagram indicates a similar traffic situlation as that in [3]. Different bounds for accelerations are reported: for instance 0.5m/s^2 - 3m/s^2 [13], or 1.5m/s^2 - 2m/s^2 [26]. We combine these and set the limits for desired accelerations from 0.5m/s^2 to 2m/s^2. We will limit the range further.

Consider a stop-and-go wave that propagates at speed w for $\tau = 10$ minutes. Variational theory [27] gives the number of vehicles in the queue $n = \left\lfloor \frac{w\rho_{\text{jam}}\tau}{60} \right\rfloor = 1320$ veh. This section analyses the queue discharge rate for this queue.

As shown in Equation (16), $E(H)$ is a function of $a_{\min}$, $a_{\max}$ and n. The sensitivity of the queue discharge rate to the average desired accelerations, standard spread of desired accelerations and number of vehicles are evaluated with Equation (16) and (17), presented in Figure 3.

Figure 3a presents a relation between the speed in congestion v_j and the queue discharge rate q_d when setting $E\left(a^{desire}\right)$ as 0.75m/s^2, 1.25m/s^2, 1.75m/s^2 respectively and $\sigma^2\left(a^{desire}\right) = \frac{0.5^2}{12}$. We obtain so by setting the pair $(a_{\min}, a_{\max})$ to (0.5m/s^2,1m/s^2), (1m/s^2,1.5m/s^2) and (1.5m/s^2, 2m/s^2). We see that the faster the average desired acceleration, the higher the queue discharge rate.

Figure 3b presents the relation between v_j and q_d when $\sigma^2\left(a^{desire}\right)$ equals to $\frac{0.5^2}{12}$, $\frac{0.9^2}{12}$ and $\frac{1.5^2}{12}$, setting $E\left(a^{desire}\right) = 1.25\text{m/s}^2$. That is, the pair $(a_{\min}, a_{\max})$ are chosen to (1m/s^2,1.5m/s^2), (0.8m/s^2,1.7m/s^2) and (0.5m/s^2,2m/s^2) respectively. It indicates that the larger the spread, the lower the queue discharge rate.

If we fix $a_{\min} = 0.5\text{m/s}^2$ and decrease $a_{\max}$ from 2m/s^2 to 1m/s^2, then both of $E\left(a^{desire}\right)$ and $\sigma^2\left(a^{desire}\right)$ decreases. Figure 3c shows that the decrease of $a_{\max}$ increases the queue discharge rates. Since the decrease of $E\left(a^{desire}\right)$ and $\sigma^2\left(a^{desire}\right)$ will decrease and increase the queue discharge rate respectively, the increase of queue discharge rates in Figure 3c indicates that $\sigma^2\left(a^{desire}\right)$ has more influences on the queue discharge rate than $E\left(a^{desire}\right)$.

Figure 3d shows the sensitivity to n with $a_{\min} = 0.5\text{m/s}^2$ and $a_{\max} = 2\text{m/s}^2$. The more vehicles, the higher queue discharge rates. It is not a surprise because the follower's acceleration is always limited by its leader's acceleration, that makes the acceleration spread decrease as the vehicle number increases. Since $n = 1320$ means the congestion only propagates for 10min, the queue discharge rate can be even higher when setting a longer time of congestion propagation.

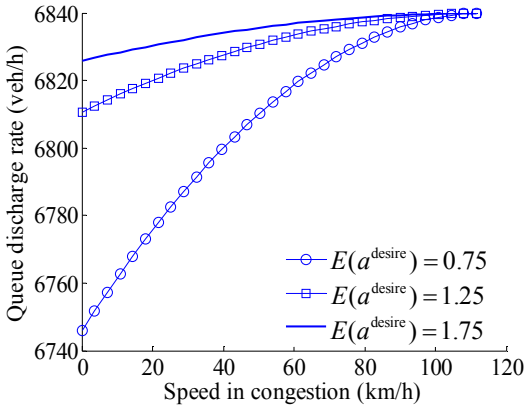

a) Sensitivity of the analytical model to the mathematic expectation of desired accelerations.

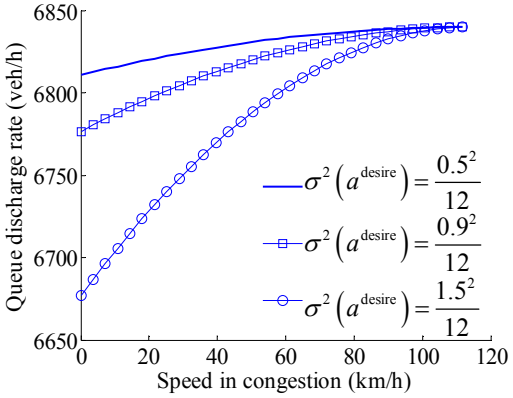

b) Sensitivity of the analytical model to the standard deviations of desired accelerations.

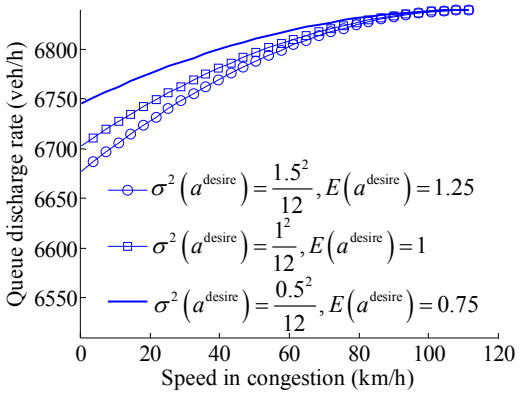

c) Comparisions of impacts on queue discharge rates between the mathematical expectation and the standard deviations of desired accelerations.

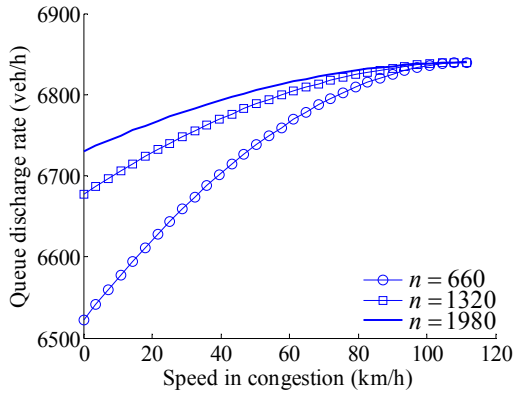

d) Sensitivity of the analytical model to the vehicle number .

Figure 3 Sensitivity of queue discharge rates when capacity drop is due to the acceleration spread.

Setting $a_{\min} = 0.5\text{m/s}^2$, $a_{\max} = 2\text{m/s}^2$ and $n = 660$ veh gives a considerable influence of the acceleration spread on queue discharge rates, shown as the line with circles in Figure 3d. However, the contribution of acceleration spread to the queue discharge rate reduction is still marginal. In Figure 3d when $v_j = 0\text{km/h}$, the minimum queue discharge rate (6522veh/h) is still much higher than the empirical value (5000veh/h) shown in Figure 1.

Note that the hypothesis about the uniform desired acceleration distribution has already maximized the $\sigma^2\left(a^{desire}\right)$. In reality, the desired acceleration could follow some distribution with peaks (such as shown in [28]) which will have smaller $\sigma^2\left(a^{desire}\right)$. Therefore, we can conclude that the acceleration spread is not a dominant factor for capacity drop.

3.2 Capacity drop due to reaction time extension

This section shows that the reaction time extension can considerably influence the queue discharge rate. A negative relation between the reaction time and the speed in congestion could result in a similar queue discharge rates as empirical findings. We give analytical expressions of queue discharge rates and the sensitivity analyses in section 3.2.1 and 3.2.2, respectively.

3.2.1 Analytical expressions of queue discharge rates

If all vehicles have the same acceleration while the reaction time of each driver is larger than Δt, the queue discharge rate will be lower than the capacity. We consider only the cases when the reaction time is longer. Therefore, we can define

$$t_r = \Delta t + \Delta t_{ex} \tag{18}$$

Δt is considered as a fixed reaction time (related to the fundamental diagram) and Δt_{ex} as a reaction time extention. As shown in Figure 2e, two bold solid lines are trajectories of two successive vehicles accelerating from speed v_j up to free speed v_f. The follower's reaction time is extended by Δt_{ex} from Δt. The dashed line is the follower's trajectory when $\Delta t_{ex} = 0$. The follower's trajectory can be considered as a shifted trajectory from the dashed line in time (by Δt_{ex}) and space (by s_{shift}). Hence,

$$v_j = \frac{s_{shift}}{\Delta t_{ex}} \tag{19}$$

$$s_i^{extension} + s_{shift} = v_f \Delta t_{ex} \tag{20}$$

So we can have:

$$s_i = \frac{1}{\rho_{\text{cri}}} + s_i^{extension} = \frac{1}{\rho_{\text{cri}}} + \left(v_f - v_j\right) \cdot \Delta t_{ex} \tag{21}$$

Consider n vehicles accelerating from a queue with the same acceleration (see Figure 2f. the spacing between the first and last vehicle is:

$$s_{1,n} = (n-1)\frac{1}{\rho_{\text{cri}}} + \sum_{i=1}^{n-1} s_i^{extension} = \frac{n-1}{\rho_{\text{cri}}} + (n-1)\left(v_f - v_j\right)\Delta t_{ex} \tag{22}$$

Hence,

$$H = \frac{s_{1,n}}{v_f} = \frac{n-1}{\rho_{\text{cri}} v_f} + \frac{(n-1)\left(v_j - v_f\right)\Delta t_{ex}}{v_f} \tag{23}$$

So the queue discharge rate equals to:

$$q_d = \frac{n-1}{H} = \frac{v_f \rho_{\text{cri}}}{1 + \rho_{\text{cri}}\left(v_j - v_f\right)\Delta t_{ex}} \tag{24}$$

3.2.2 Analysis of model properties

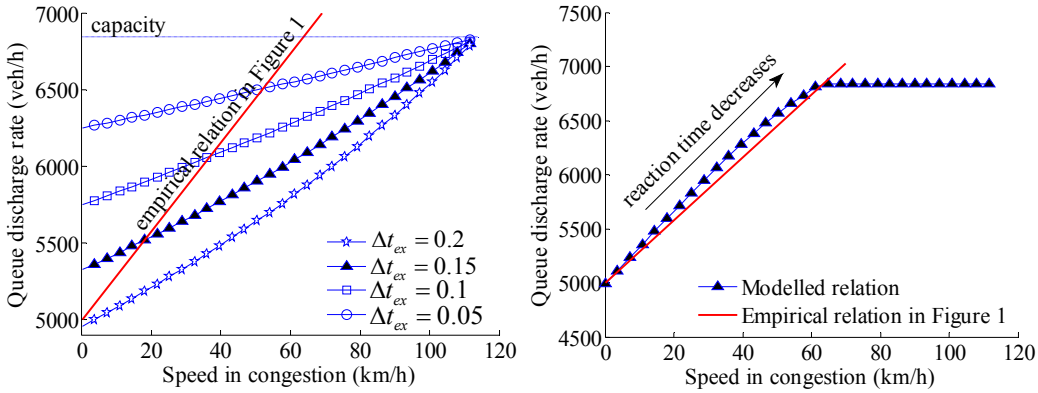

a) Sensitivity of the analytical model to the reaction time extension

b) An intra-driver reaction time extension mechanism for giving empirical observations

Figure 4 Sensitivity of queue discharge rates to reaction time extensions

The independent impact of the reaction time extension is evalued with Equation (24), see Figure 4a. We examine the relation between the speed in cognestion and the queue discharge rate, setting reaction time extension Δt_{ex} to 0.05s, 0.1s, 0.15s and 0.2s. Figure 4a firstly indicates that reaction time extension Δt_{ex} can give a positive relation between the speed in congestion and the queue discharge rate. As the reaction time extension increases even slightly, the queue discharge rate will decrease considerably. When $\Delta t_{ex} = 0\text{s}$, the queue discharge rate equals to the capacity. Secondly, a dynamic reaction time extension can model the empirical observation. The bold line in Figure 4a is the empirical relation revealed in [3] (see Figure 1). The intersections between the bold line and the other lines indicates that to give empirical observations we may need to decrease the reation time extension as the speed in congestion increases. When the vehicular speed in queue reached around 63km/h, there is no capacity drop. That is, the reaction time

extension might be zero. We use $v_j^{\max}$ to indicate the lowest speed in congestion leading to no capacity drop. Hence, we set

$$\Delta t_{ex} = \max\left(0, \gamma - \frac{\gamma v_j}{v_j^{\max}}\right) \quad (25)$$

γ is a parameter indicating the reaction time extension when the speed in congestion is 0 km/h. Varying with γ, we find a good relationship if we set $\gamma = 0.195\text{s}$. The modelled realtion with Equation (25) is shown as dark triangulars in Figure 4b. The bold line is the empirical realtion as in Figure 1. The modelled relation can fit the empirical relation quite well, see Figure 4b.

4. Numerical experiments

In this section, we use numerical experiments to firstly validate the analytical model presented in section 3.1.1. The estimation of queue discharge rate is an approximation. So we need to check whether the approximation is accurate enough. This validation step aims to make our conclusions solid.

Secondly, we present the combination effects of bounded acceleration spread and the reaction time extensions. A positive reaction time extension can allow a following vehicle to have a faster-than-predecessor acceleration. So the acceleration of the last vehicle in the queue will not follow Equation (8) any more, i.e., a_n does not have to be the slowest acceleraion among all vehicles in the queue. The distribution of the last vehicle's acceleration is difficult to deduce, so we decide to use numerical experiments to see the combination effects of bounded acceleration spread and the reaction time extensions.

Thirdly, we try to see how to give a same relation between the speed in congestion and the queue discharge rate as empirical observations, considering combination effects of the acceleration spread and the reaction time extension.

The simulation results in this section correlate quite well with our analytical findings in section 3. No matter whether the reaction time is included or not, the acceleration spread does not contribute sufficiently to the capacity drop. No matter whether the acceleration spread is considered, a negative relation between the reaction time and the speed in congestion can give similar queue discharge rates as empirical observations.

4.1 Simulation model used

Figure 5 shows trajectories of two vehicles accelerating from congestion. Vehicle $i-1$ is the leader of vehicle i. Let us set an acceleration difference Δa. The free-flow spacing between Vehicle i and $i-1$ will be $\frac{1}{\rho_{cri}}$ if $a_i = a_{i-1} + \Delta a$ .So if $a_i > a_{i-1} + \Delta a$, the free-

flow spacing between two vehicles will be smaller than the critical spacing $\frac{1}{\rho_{cri}}$. In Figure 5 we use a dashed line to present a trajectory of vehicle i according to Newell's model.. Finally the trajectory of vehicle i will ovaerlap with the dashed line. Vehicle i reached the free-flow speed earlier than the dashed trajectory by Δt_2. The whole acceleration process of vehicle i last Δt_1. Hence, we can have:

$$v_f = v_j + a_{i-1}\left(\Delta t_{ex} + \Delta t_1 + \Delta t_2\right) \tag{26}$$

$$v_f = v_j + \left(a_{i-1} + \Delta a\right)\Delta t_1 \tag{27}$$

$$v_f = \frac{\frac{v_f^2 - v_j^2}{2a_{i-1}} - \left(v_j \Delta t_{ex} + \frac{v_f^2 - v_j^2}{2\left(a_{i-1} + \Delta a\right)}\right)}{\Delta t_3} \tag{28}$$

Equation (26) and (29) describe the acceleration process of the dashed trajectory and vehicle i, respectively. Equation (28) means finally vehicle i will overlap the dashed trajectory when $a_i = a_i^{\text{desire}} = a_{i-1} + \Delta a$.

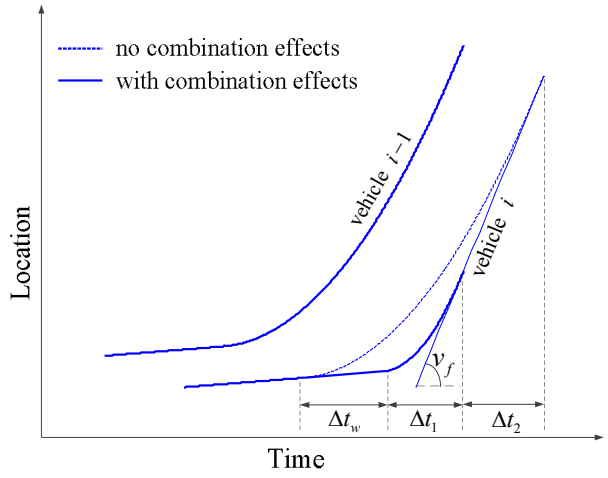

Figure 5 Measurement of accelerations when reaction time is extended.

Combination of Equation (26) - (28) can give:

$$\Delta a = \frac{2a_{i-1}^2 \Delta t_{ex}}{v_f - v_j - 2a_{i-1}\Delta t_{ex}}, \quad \text{for} \quad v_f - v_j > 2a_{i-1}\Delta t_{ex} \tag{29}$$

Equation (29) shows that the following vehicle can catch up with its predecessor with $a_i = a_{i-1} + \Delta a$ when $v_f - v_j > 2a_{i-1}\Delta t_{ex}$. If $a_{i-1} + \Delta a \le a_i^{\text{desire}}$, then $a_i = a_{i-1} + \Delta a$, the free-flow spacing between vehicle i and $i-1$ will be critical spacing. If $a_{i-1} + \Delta a > a_i^{\text{desire}}$, then $a_i = a_i^{\text{desire}} < a_{i-1} + \Delta a$, the free-flow spacing between two successive vehicles are:

$$s_i = \frac{1}{\rho_{cri}} + \frac{\left(\frac{1}{a_i} - \frac{1}{a_{i-1}}\right)\left(v_j - v_f\right)^2}{2} + \left(v_f - v_j\right)\Delta t_{ex} \tag{30}$$

When $v_f - v_j \le 2a_{i-1}\Delta t_{ex}$, i.e., the reaction time is too long, and it is impossible for the follower to catch up with the leader. In the this case, the follower's acceleration will not be limited by its predecessor, i.e., $a_i = a_i^{\text{desire}}$. The free-flow spacing between two vehicles will be larger than the critical spacing, calculated according to Equation (31). In summary:

$$a_i = \min\left(a_{i-1} + \Delta a, a_i^{\text{desire}}\right) \tag{31}$$

$$s_i = \begin{cases} \dfrac{1}{\rho_{cri}}, & \text{for } v_f - v_j > 2a_{i-1}\Delta t_{ex} \text{ and } a_{i-1} + \Delta a \le a_i^{\text{desire}} \\ \dfrac{1}{\rho_{cri}} + \dfrac{\left(\frac{1}{a_i} - \frac{1}{a_{i-1}}\right)\left(v_j - v_f\right)^2}{2} + \left(v_f - v_j\right)\Delta t_{ex}, & \text{otherwise} \end{cases} \tag{32}$$

Finally, in the numerical experiment we calculate the queue discharge flow as:

$$q_d = \frac{v_f}{E\left(s_i\right)}, \quad i = 2, \ldots, n \tag{33}$$

Equation (32) and (33) are general expressions for estimating queue discharge rates in the three experiments, that is for the validation of analytical models, the examination of combination effects and the reproduction of empirical observations respectively.

Since in section 3.1, we found the independent impact of acceleration on the queue discharge rate is marginal. We hypothesize that when considering reaction time extensions, the acceleration spread cannot contribute to queue discharge rate reduction greatly, either. The consequence of the hypothesis is that to obtain the empirically observed queue discharge rate (Figure 1), it is more important to model the impact of the reaction time extension than that of the acceleration spread. Hence, we still use Equation (25) to give the queue discharge rate.

4.2 Simulation set-up

For validations of the analytical model in section 3.2.1, we let $\Delta t_{ex} = 0\text{s}$. For examining combination effects of the acceleration spread and the reaction time extension, we set two scenarios, i.e., $\Delta t_{ex} = 0.1\text{s}$ and $\Delta t_{ex} = 0.2\text{s}$. Finally, in the third experiment we give $\gamma = 0.18\text{s}$.

At the beginning of the experiment, we set all vehicles' desired acceleration and reaction time extension. With Equation (31) - (33), we can directly have the final queue discharge rate. The notations of models and the set-up of fundamental diagram are the same as those in section 3. To draw the relation between the speed in congestion and the queue discharge rate, in each scenario set-up we run one simulation with newly distributed

desired accelerations for each speed in congestion. We run the simulation for 1000 times to get the expected value and standard spread of queue discharge rates. we set $n = 660\text{veh}$, $a_{\min} = 0.5\text{m/s}^2$ and $a_{\max} = 2\text{m/s}^2$.

4.3 Validations of analytical models

We approximate the mean queue discharge rate by approximating the expected value of the time-headway in section 3.1. So we need to check whether the approximations are accurate enough to draw conclusions on the independent impacts of accelerations. The comparison between the numerical experiment result and the analytical result is shown in Figure 6a. In Figure 6a, we use error bars and plus signs to indicate the standard spread and the expected value of queue discharge rates respectively for experiment results. Circles show the analytical approximations of queue discharge rates from section 3.1.1.

We find that the analytical approximations of queue discharge rates fit the numerical experiment results well. Secondly, the queue discharge rate spread increases as the speed in congestion decreases. The fluctuation of queue discharge rate might be a related to the order of desired accelerations. But the spread is not high. All in all, the analysis of the independent impacts of accelerations on the queue discharge rate in section 3.1 is correct.

4.4 Combination effects of the accelerations spread and reaction time extension

The combination effects of the acceleration spread and the reaction time extension is examined in numerical experiments, shown in Figure 6b. The experiment results, i.e., mean and standard spreads of queue discharge rates, are shown as plus signs and error bars in Figure 6b, respectively. As a reference, we use circles to indicate the mean queue discharge rate with the independent impact of reaction time, which is the same as shown in Figure 4a.

In Figure 6b, the acceleration spread hardly contribute to the queue discharge rate reduction. The maximum reduction in experiments is 180 vehicles (around 3% reduction) when $\Delta t_{ex} = 0.1\text{s}$ and $v_j = 0\text{km/h}$. Meanwhile, increasing Δt_{ex} from 0.1s to 0.2s decreases the queue discharge rate considerably. When $v_j = 0\text{km/h}$, the queue discharge rate decreases around 13% (with acceleration spread) and 14% (without acceleration spread). It also means a slight decrease of reaction time can contribute a considerable increase of queue discharge rates.

Because the acceleration spread can only reduce the queue discharge rate slightly, we use Equation (25) to model mechanism of capacity drop to give queue discharge rates. The experiment results are in Figure 6c. As reaction time decreases when congestion gets lighter, queue discharge rates can fit empirical observations well.

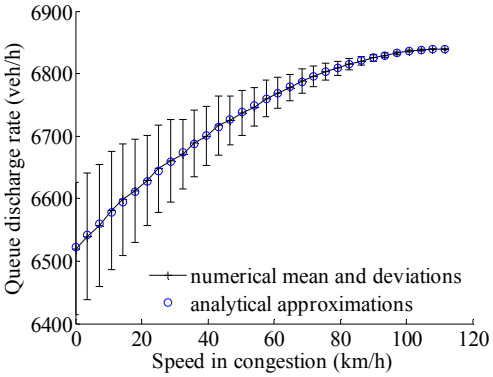

a) Validation of the analytical model for the inter-driver acceleration spread

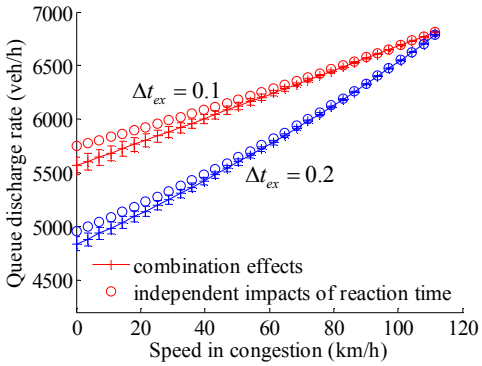

b) Combination effects of inter-driver acceleration spread and reaction time extension on queue discharge rates

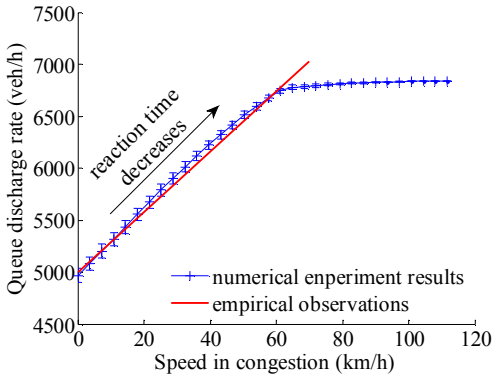

c) Combination effects on queue discharge rates with intra-driver reaction time extension mechanism

Figure 6 Results in experiments

6 CONCLUSIONS

This paper reveals the impacts of bounded accelerations and reaction time on the queue discharge rate. Firstly, we find the impact of inter-driver acceleration spread on the queue discharge rate is rather small. No matter whether the reaction time is considered or not, the acceleration spread can hardly decrease the queue discharge rate. Secondly, a speed-dependent reaction time extension mechanism, that is the reaction time decreases as the speed in congestion increases, yields a similar relation between the speed in congestion and the queue discharge rate as found in empirical observations.

Therefore, we conclude that including the acceleration spread when modelling the capacity drop within car-following models is not essential, but including reaction time variations is. Also, this paper gives reasons to believe that a control approach motivating drivers accelerate earlier might be able to considerably benefit maximizing queue discharge rates.

ACKNOWLEDGEMENTS

This research is financially supported by China Scholarship Council (CSC) and the NWO grant "There is plenty of room in the other lane".

REFERENCES

1. Chung, K., J. Rudjanakanoknad, and M.J. Cassidy, *Relation between traffic density and capacity drop at three freeway bottlenecks.* Transportation Research Part B: Methodological, 2007. **41**(1): p. 82-95.
2. Yuan, K., V.L. Knoop, L. Leclercq, and S.P. Hoogendoorn. *Capacity drop: a comparison between stop-and-go wave and queue congestion at lane-drop bottleneck*. in *Symposium celebrating 50 years of traffic flow theory*. 2014. Portland, Oregon, U.S.A.
3. Yuan, K., V.L. Knoop, and S.P. Hoogendoorn. *Capacity Drop: A Relation Between The Speed In Congestion And The Queue Discharge Rate*. in *the 94th Annual Meeting of the Transportation Research Board*. 2015. Washington D.C.
4. Oh, S. and H. Yeo, *Impact of stop-and-go waves and lane changes on discharge rate in recovery flow.* Transportation Research Part B: Methodological, 2015. **77**(0): p. 88-102.
5. Srivastava, A. and N. Geroliminis, *Empirical observations of capacity drop in freeway merges with ramp control and integration in a first-order model.* Transportation Research Part C: Emerging Technologies, 2013. **30**(0): p. 161-177.
6. Oh, S. and H. Yeo, *Estimation of Capacity Drop in Highway Merging Sections.* Transportation Research Record: Journal of the Transportation Research Board, 2012. **2286**(-1): p. 111-121.
7. Papageorgiou, M., I. Papamichail, A.D. Spiliopoulou, and A.F. Lentzakis, *Real-time merging traffic control with applications to toll plaza and work zone management.* Transportation Research Part C: Emerging Technologies, 2008. **16**(5): p. 535-553.
8. Hall, F.L. and K. Agyemang-Duah, *Freeway Capacity Drop and The Definition of Capacity.* Transportation Research Record, 1991(1320): p. 8.
9. Banks, J.H., *Two-capacity phenomenon at freeway bottlenecks: a basis for ramp metering?* Transportation Research Record, 1991(1320): p. 8.
10. Cassidy, M.J. and R.L. Bertini, *Some traffic features at freeway bottlenecks.* Transportation Research Part B: Methodological, 1999. **33**(1): p. 25-42.
11. Cassidy, M.J. and J. Rudjanakanoknad, *Increasing the capacity of an isolated merge by metering its on-ramp.* Transportation Research Part B: Methodological, 2005. **39**(10): p. 896-913.

12. Laval, J.A. and C.F. Daganzo, *Lane-changing in traffic streams*. Transportation Research Part B: Methodological, 2006. **40**(3): p. 251-264.
13. Leclercq, L., J.A. Laval, and N. Chiabaut, *Capacity drops at merges: An endogenous model.* Transportation Research Part B: Methodological, 2011. **45**(9): p. 1302-1313.
14. Leclercq, L., V.L. Knoop, F. Marczak, and S.P. Hoogendoorn. *Capacity drops at merges: New analytical investigations*. in *Intelligent Transportation Systems (ITSC), 2014 IEEE 17th International Conference on*. 2014.
15. Coifman, B. and S. Kim, *Extended bottlenecks, the fundamental relationship, and capacity drop on freeways*. Transportation Research Part A: Policy and Practice, 2011. **45**(9): p. 980-991.
16. Chen, D., S. Ahn, J. Laval, and Z. Zheng, *On the periodicity of traffic oscillations and capacity drop: The role of driver characteristics.* Transportation Research Part B: Methodological, 2014. **59**(0): p. 117-136.
17. Wong, G. and S. Wong, *A multi-class traffic flow model–an extension of LWR model with heterogeneous drivers.* Transportation Research Part A: Policy and Practice, 2002. **36**(9): p. 827-841.
18. Coifman, B., S. Krishnamurthy, and X. Wang, *Lane-Change Maneuvers Consuming Freeway Capacity*, in *Traffic and Granular Flow '03*, S. Hoogendoorn, et al., Editors. 2005, Springer Berlin Heidelberg. p. 3-14.
19. Treiber, M., A. Kesting, and D. Helbing, *Understanding widely scattered traffic flows, the capacity drop, and platoons as effects of variance-driven time gaps.* Physical Review E, 2006. **74**(1): p. 016123.
20. Zhang, H.M. and T. Kim, *A car-following theory for multiphase vehicular traffic flow.* Transportation Research Part B: Methodological, 2005. **39**(5): p. 385-399.
21. Yeo, H., *Asymmetric Microscopic Driving Behavior Theory*. 2008.
22. Tampère, C., *Human-kinetic multiclass traffic flow theory and modelling with application to advanced driver assistance systems in congestion*. Vol. PhD. 2004, The Netherlands: Delft University of Technology.
23. Nishinari, K., M. Treiber, and D. Helbing, *Interpreting the wide scattering of synchronized traffic data by time gap statistics*. Physical Review E, 2003. **68**(6): p. 067101.
24. Newell, G.F., *A simplified car-following theory: a lower order model.* Transportation Research Part B: Methodological, 2002. **36**(3): p. 195-205.
25. Reiss, R.-D., *Approximate Distributions of Order Statistics: with applications to nonparametric statistics*. 1989, New York: Springer-Verlag.
26. Lebacque, J., *Two-Phase Bounded-Acceleration Traffic Flow Model: Analytical Solutions and Applications*. Transportation Research Record: Journal of the Transportation Research Board, 2003. **1852**: p. 220-230.
27. Daganzo, C.F., *A variational formulation of kinematic waves: basic theory and complex boundary conditions*. Transportation Research Part B: Methodological, 2005. **39**(2): p. 187-196.
28. Koutsopoulos, H.N. and H. Farah, *Latent class model for car following behavior.* Transportation Research Part B: Methodological, 2012. **46**(5): p. 563-578.